scientific reports

Check for updates

OPEN

Early warning method for charging thermal runaway of electric vehicle lithium-ion battery based on charging network

Yuan-Ming Cheng[1], De-Xin Gao[1]✉, Feng-Ming Zhao[1] & Qing Yang[2]

New energy vehicles are becoming a new trend in global transportation development due to the renewable and environmentally friendly nature of the fuel they consume. At the same time, the charging safety of electric vehicle (EV) lithium-ion battery limits the development of the industry. This paper obtains charging data through the EV charging network, takes the lithium-ion battery charging temperature as the observation value, and proposes an early warning method for EV lithium-ion battery based on the charging network according to the nonlinear relationship between the temperature and the charging voltage, current, and battery status. First, we obtain the charging data through the charging network, select the model input parameters, and establish the long- and short-term memory network and temporal convolutional network (LSTM-TCN) model to predict the EV charging temperature. Then, compare the real-time charging data with the predicted data to get the model with the highest accuracy, and analyze the residuals by using the sliding-window method to get the pre-warning thresholds. Finally, by monitoring and calculating the changes in residuals, a thermal runaway warning system is implemented for lithium-ion battery charging to ensure the safety of EV charging. The experimental results show that the LSTM-TCN charging early warning model has higher accuracy compared with other models, which makes the method able to accurately and quickly react to charging accidents and achieve the early warning effect.

Keywords Electric vehicle, Lithium-ion battery, Thermal runaway, Safety warning, Time convolution network, Long-short memory network

The rapid development of EV makes lithium-ion battery technology a central element in driving the e-mobility revolution[1]. For the EV, the power battery system is the main source of power for EVs, and its charging and discharging current can be as high as hundreds of amperes, higher charging and discharging currents, will lead to a rapid rise in the internal temperature of the battery[2], and if the temperature can not be effectively monitored, it will accelerate the decline in battery performance or even lead to safety accidents such as thermal runaway of the battery[3]. According to statistics, in the natural accidents of EV, the thermal runaway of lithium-ion battery charging accounts for one-third of the total accidents, and some of the electric vehicle lithium battery thermal runaway accidents are shown in Table 1. Excessive charging temperature may lead to serious consequences such as battery damage, performance degradation and even fire[4], so real-time monitoring and prediction of the risk of thermal runaway during battery charging is crucial to ensure the safe operation of EV.

At present, researchers at home and abroad have carried out a lot of exploration on the thermal runaway problem of lithium-ion battery, including experimental exploration, mechanism analysis, and safety protection[5–7], and have preliminarily understood the triggering mechanism of thermal runaway[8,9], the expansion mechanism, and the warning method of safety protection[10,11], which lays the foundation for the large-scale promotion and application of EV[12,13]. At this stage, there are three main directions to solve the thermal runaway problem of lithium-ion battery charging in EV, namely, material improvement[14–16], battery modeling[17–19], and big data prediction[20–22].

Early researchers utilized phase change materials to replace the internal cooling system of cylindrical battery hollow core rods[15]. The research results indicated that this system exhibited significant cooling effectiveness. However, the process of material development and replacement may present complexities. To reduce research

[1]Department of Automation and Electronic Engineering, Qingdao University of Science and Technology, Qingdao 266061, China. [2]Department of Computer Science and Technology, Qingdao University of Science and Technology, Qingdao 266061, China. ✉email: gaodexin@qust.edu.cn

No	Time	Site	Accident analysis
1	2016.01	Järsta, Norway	Spontaneous combustion caused by prolonged exposure of batteries to cold temperatures
2	2019.04	Shanghai, China	Failure of a single cell, resulting in a short circuit of the battery
3	2019.01	Antwerp, Belgium	Charging short circuit fault
4	2019.01	Daegu, Korea	The interior of the power battery assembly started the fire
5	2020.05	Dongguan, China	Battery pack with charging fault problem
6	2020.08	Guangzhou, China	EV overcharging caused short circuit problems inside batteries
7	2021.02	Hohhot, China	Spontaneous combustion of high-voltage batteries, causing spontaneous combustion in other vehicles
8	2021.08	Guangzhou, China	Battery damage due to collision
9	2022.09	Telangana, India	Short-circuit problems due to overcharging of EV
10	2022.01	Florida, USA	Short-circuit problems caused by water immersion in car battery packs
11	2023.03	Taiyuan, China	Spontaneous combustion caused by overheating of the battery while charging
12	2023.07	Dongguan, China	Broken Battery Causes Spontaneous Combustion
13	2023.01	Plano, USA	Battery Failure Sudden Spontaneous Combustion

Table 1. EV lithium-ion battery charging thermal runaway accident table.

and development costs, the establishment of lithium-ion battery models has become a primary approach for studying battery characteristics[17]. In practical applications, the construction of electric vehicle lithium-ion battery models primarily adopts comprehensive models, including the establishment of equivalent circuit models[18], conjugate heat transfer models, and reaction kinetics models[19]. Through numerical simulations, multiple features are extracted to enable early warning of battery faults. However, there are delay defects in the sensors and the battery model construction is complicated, so the intelligent management of lithium-ion battery charging through big data has become the main way to ensure the safety of EV charging.

With the development of deep learning, combined with the nonlinear characteristics of the EV lithium-ion battery charging process, the deep learning network is applied in the field of EV lithium-ion battery fault early warning, for the integration of big data and new energy vehicles, provides a solid foundation. Based on previous studies utilizing characteristic signals of lithium-ion batteries for fault identification and diagnosis, existing big data-driven early warning methods integrate both external and internal parameters-such as surface temperature, terminal voltage, internal impedance, expansion force, and gas generation[20–22]. By combining these parameters, models can be trained to predict key indicators of thermal runaway, ultimately achieving reliable early warning outcomes[23] employed a convolutional neural network (CNN) to classify and predict three distinct stages-safe operation, the critical pre-thermal runaway condition, and the actual thermal runaway occurrence-to prevent thermal runaway in lithium-ion batteries[24] proposed a CNN and bidirectional recurrent neural network (BiGRU) based EV charging state monitoring and safety warning method, and the experimental results show that the method phase has higher prediction accuracy and prediction effect.

Although existing deep learning models can provide early warning of thermal runaway during the charging process of lithium-ion batteries in EVs, their accuracy still requires improvement, and the warning system needs further refinement. Based on the above research results, this paper proposes a thermal runaway early warning method for EV lithium-ion battery charging, based on a charging network. With battery temperature as the target observation, an LSTM-TCN temperature prediction model is constructed. A sliding window combined with residual analysis is employed to monitor the predicted and actual charging temperatures, and an early warning threshold is established to achieve effective thermal runaway prevention. The main contents of this paper are as follows:

(1) The prediction accuracy is further improved by developing a hybrid LSTM-TCN prediction model based on the temporal characteristics of lithium-ion battery charging data.
(2) Determine the warning threshold and enhance the reliability of early warning through residual analysis and monitoring of temperature residuals.
(3) The generalizability of the proposed warning method is demonstrated through experimental validation using normal and abnormal charging data from two different types of EV lithium-ion batteries at varying temperatures.

The remaining chapters of this paper are organized as follows: the second part analyzes the thermal runaway of lithium-ion battery, including the reasons for the departure of the thermal runaway, the description of the stages, and the behavioral characteristics; the third part briefly describes the charging standards of lithium-ion battery for EV, preprocesses the experimental data, completes the construction of the prediction model, and carries out the design of the thermal runaway warning process. The fourth part describes and analyzes the overall experiment, first prepares the experiment, then uses different data to conduct the experiment and analyze the results. Chapter "Conclusion" summarizes the article.

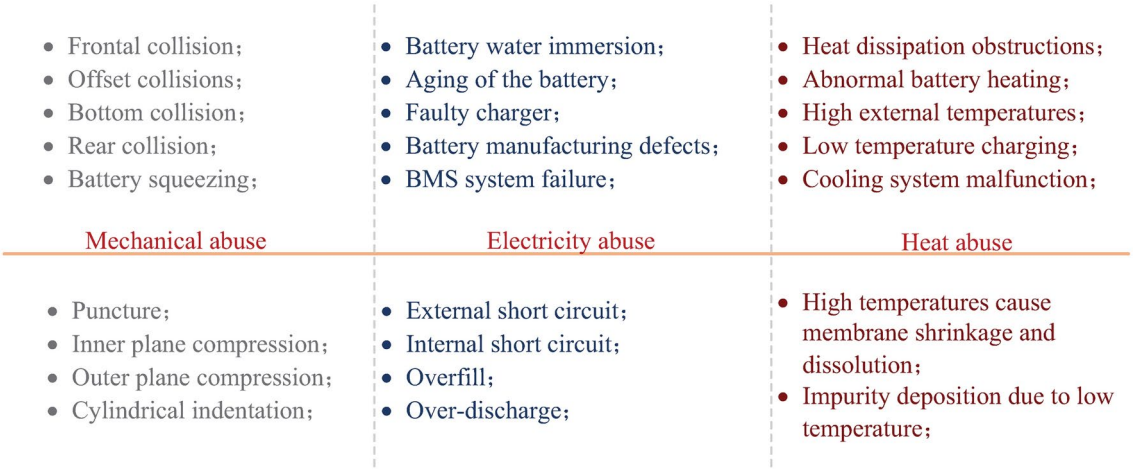

Fig. 1. Lithium-ion battery charging thermal runaway trigger conditions.

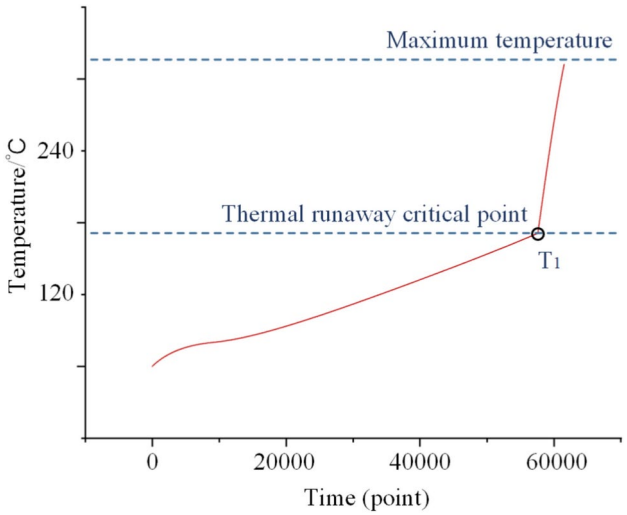

Fig. 2. Thermal runaway temperature variation.

Lithium-ion battery thermal runaway analysis

Lithium-ion battery charging thermal runaway trigger causes

EV lithium-ion battery is subject to internal and external factors with uncertainties during the charging process in the charging network, some of which can cause damage to the battery system, thus increasing the risk of thermal runaway charging[25]. Among them, internal factors are mainly battery aging, battery manufacturing defects, and EV BMS failures[26,27]; external factors are mainly caused by violent collisions, battery flooding, and external high and low temperatures[28,29]. The lithium-ion battery thermal runaway triggering conditions are categorized into three types: mechanical abuse, electrical abuse and thermal abuse[30], and the specific causes of failure are shown in Fig. 1. Due to these unavoidable factors, the lithium-ion battery generates excessive heat inside the battery during the charging process, which leads to an increase in battery temperature and triggers serious safety problems such as fire and explosion[31]. Therefore, it is of great significance to propose a reasonable early warning method by studying the thermal runaway mechanism of EV lithium-ion battery.

Lithium-ion battery thermal runaway stage division

When thermal runaway occurs in lithium-ion battery, the most direct manifestation is a rapid increase in temperature, accompanied by extreme situations such as possible fire and explosion[32]. The instant thermal runaway occurs, the internal temperature of the battery increases dramatically, as shown in Fig. 2. Thermal runaway occurs in electric vehicle lithium batteries during the charging process, which is usually divided into four stages[33].

The first stage is the battery overcharging stage, which may occur during the battery charging process due to internal battery factors, failure of the charge control system, or improper operation, which may cause the battery

to continuously receive electrical energy[34]. Overcharging will lead to excessive gas generation and pressure rise inside the battery, which will trigger safety hazards.

The second stage is the overheating stage, which may be triggered when the internal temperature of the battery exceeds the safety limit. Overheating will lead to changes in the internal materials of the battery, increasing the risk of thermal runaway, and may trigger a chain reaction of thermal runaway. As shown in Fig. 2, the temperature reaching point T1 in the overheating stage is the critical temperature at which thermal runaway occurs, and if we want to block thermal runaway from occurring, we have to warn and take measures before the temperature reaches T1[35].

The third section of the stage is the thermal runaway stage, that is, the dotted line interval shown in Fig. 2. On the basis of overheating, if the chemical reaction inside the battery is out of control, it may trigger more serious thermal runaway phenomena, including smoke, flame, and even explosion[36]. This stage of thermal runaway phenomenon may spread rapidly, posing a serious threat to the vehicles and the surrounding environment.

The fourth stage is the diffusion stage, once the thermal runaway occurs, it may lead to the successive loss of control of other single batteries within the battery pack, forming a chain reaction, so that the scope of the accident is expanded, causing a greater impact on safety.

These four stages constitute the key stages in which thermal runaway may occur in the charging process of EV lithium-ion battery, and these risks need to be prevented and avoided through scientific management and control measures.

Lithium-ion battery charging safety management and thermal runaway warning

EV lithium-ion battery charging network charging process reference basis

At present, the charging process of EV lithium-ion battery has a variety of reference specifications. Among them, the Specification for Battery System Safety Risk Monitoring and Failure Early Warning for Electric Vehicle Charging Process (T/CSAE 254-2022) analyzes the current situation of the EV charging process. It uses charging big data analysis to propose requirements for the charging system and safety early warning methods. This specification aims to take the charging process as a perspective to discover charging anomalies[37]. It also seeks to provide relevant early warnings before serious safety risks arise, allowing charging big data to play an effective role.

According to the standards stipulated in T/CSAE 254-2022, the charging process of EV needs to confirm the parameters and status of the charging equipment, including the input voltage, current and frequency, and the output voltage, current and power, to ensure the stability and safety of the charging process. At the same time, the physical connection and communication protocol of the charger and charging interface need to be tested to ensure the reliability and operability of the charging process. The charging information table of the whole EV is shown in Table 2.

Data projects	Description and requirements	Charging stage
Rated capacity of whole vehicle power battery system (Ah)	Data resolution: 0.1Ah/bit, 0Ah offset;	Handshake phase
Rated total voltage of power battery system of the whole vehicle (V)	Data resolution: 0.1V/bit, 0V offset;	
Maximum permissible total charging voltage (V)	Data resolution: 0.1V/bit, 0V offset;	Parameter configuration phase
Maximum allowable charging current (A)	Data resolution: 0.1A/bit, − 400A offset;	
Maximum permissible temperature (°C)	Data resolution: 1°C/bit, − 50 °C offset;	
	Data range: − 50 °C to +200°C;	
Vehicle power battery charge state (%)	Data resolution: 0.1%/bit, 0% offset;	
	Data range: 0–100%;	
Measured charging voltage (V)	Data resolution: 0.1V/bit, 0V offset;	Recharge phase
Measured charging current (A)	Data resolution: 0.1A/bit, − 400A offset;	
Maximum power battery temperature (°C)	Data resolution: 1°C/bit, − 50 °C offset;	
	Data range: − 50 °C to +200°C;	
Minimum power battery temperature (°C)	Data resolution: 1°C/bit, − 50 °C offset;	
	Data range: − 50 °C to +200°C;	
Minimum voltage of power battery unit (V)	Data resolution: 0.1V/bit, 0V offset;	End-of-charge phase
	Data range: 0-24V;	
Maximum voltage of power battery unit (V)	Data resolution: 0.1V/bit, 0V offset;	
	Data range: 0-24V;	
Maximum temperature of power battery (°C)	Data resolution: 1°C/bit, − 50 °C offset;	
	Data range: − 50 °C to +200°C;	
Minimum temperature of power battery (°C)	Data resolution: 1°C/bit, − 50 °C offset;	
	Data range: − 50 °C to +200°C;	

Table 2. The main state information of EV lithium-ion battery before charging.

Multi-parameter selection and pre-processing

In the EV lithium-ion battery charging network power process, the charging temperature change is affected by many factors. In order to select appropriate experimental data, we use the correlation coefficient method to calculate the correlation between each charging parameter and charging temperature, the calculation formula is as follows:

$$r = \frac{\sum (E_t - \bar{E})(F_t - \bar{F})}{\sqrt{\sum_{t=1}^{n} (E_t - \bar{E})^2} \sqrt{\sum_{t=1}^{n} (F_t - \bar{F})^2}} \tag{1}$$

where r is the obtained correlation coefficient, with the value ranging from [− 1,1]; n is the total number of charging data; E_t and F_t are the real-time charging data at time t ; $\bar{E}$ and $\bar{F}$ are the average. The closer the absolute value of the obtained correlation coefficient r is to 1, the higher the correlation between E and F is[38].

After calculation, the six parameters of charging demand voltage, demand current, lithium-ion battery cell voltage, actual charging voltage, actual charging current, and battery state of charge (SOC) are selected as model inputs. The specific correlation coefficient values are shown in Table 3. Where, RequireU and RequireI are the voltage and current levels required by the battery during the charging process, typically set based on the battery's characteristics and charging strategy. SingleU refers to the voltage of an individual battery cell. ChargeU and ChargeI are the voltage and current supplied to the battery during the actual charging process. SOC is the state of charge of the battery. In the correlation coefficients presented in Table 3, the absolute values of the selected charging data's correlation coefficients with charging temperature are all greater than 0.5, indicating a strong correlation with charging temperature. Furthermore, RequireU, SingleU, ChargeU, and SOC exhibit a positive correlation with temperature, while RequireI and ChargeI show a negative correlation with charging temperature.

According to the type of charging data, the resulting data set is preprocessed. Since the EV lithium-ion battery will cause the missing data obtained during the charging process due to the influence of hardware and environmental factors, the interpolation method is used to fill in the missing data[39]. It estimates the missing values through the function relationship between the known data, and the specific calculation formula is as follows:

$$x_a = x_0 + \frac{x_1 - x_0}{p_1 - p_0}(p - p_0) \tag{2}$$

where p is the missing charging data point, p_0 and p_1 are the known data points before and after p respectively, x_0 and x_1 are the charging data values corresponding to p_0 and p_1 respectively, x_a is the data value required for interpolation.

Since the charging parameters used in this paper have different scales and value ranges, the data set is normalized in order to speed up the convergence of the model and improve the stability of the model. The specific equations are as follows:

$$x_{norm} = \frac{x - x_{\min}}{x_{\max} - x_{\min}} \tag{3}$$

where x is the original dataset, $x_{\min}$ and $x_{\max}$ are the maximum and minimum values in the data, x_{norm} is the normalized data which is used as an input to the deep model network.

In this paper, charging data such as voltage, current, and temperature of charging piles, as well as on-board lithium-ion batteries, are collected through the EV charging network. The cycle-type data of charging lithium-ion batteries for two types of EVs are obtained by referencing T/CSAE 254-2022, which is the Specification for Safety Risk Monitoring and Fault Early Warning of Battery Systems in Electric Vehicle Charging Processes. This dataset is used in this experiment to validate the practicability of the proposed method.

Lithium-ion battery charging temperature prediction model construction

The LSTM-TCN model takes the temperature-related parameters such as EV lithium-ion battery charging demand voltage, demand current, and cell voltage as input data, extracts the short-time features through the LSTM network[40], and then obtains the long-term time-series features through the TCN network[41], and at the same time captures the long-term dependence and the local correlation in the time-series data, to better

No	Data name	Correlation coefficient with temperature
1	RequireU	0.83
2	RequireI	− 0.54
3	SingleU	0.84
4	ChargeU	0.82
5	ChargeI	− 0.52
6	SOC	0.98

Table 3. Table of correlation coefficients for EV charging data.

understand the long-term trend of the temperature change and the short-term fluctuation, so as to the LSTM-TCN structure is shown in Fig. 3.

LSTM network is a special type of recurrent neural network (RNN) with a special structural design that allows it to avoid the long-term dependency problem and remember information from earlier moments[42]. The key to the LSTM is the cell states, each of which controls the retention and transfer of information in the LSTM by means of forgetting gates, input gates, and output gates[43] as shown by dashed portions of Fig. 3.

The current LSTM receives the cell state C_{t-1} from the previous one moment and acts together with the current EV lithium-ion battery charging data input x_t to generate a new cell state C_t. In this process, a forgetting gate is first used to determine the retention and forgetting of the information in C_{t-1}, with the following formula:

$$f_t = \sigma(W_f \cdot [h_{t-1}, x_t] + b_f) \tag{4}$$

where f_t represents the output of the forget gate, with a range of [0, 1], indicating the retention ratio of each information unit within the cell state, σ is the Sigmoid activation function, W_f represents the weight matrix of the forget gate, h_{t-1} stands for the hidden state from the previous time step, x_t is the input at the current time step, and b_f is the bias term of the forget gate.

Then, an input gate determines the information to be retained in the current input x_t with the following formula:

$$i_t = \sigma(W_i \cdot [h_{t-1}, x_t] + b_i) \tag{5}$$

$$\tilde{C}_t = \tanh(W_c \cdot [h_{t-1}, x_t] + b_c) \tag{6}$$

where i_t is the output of the input gate, indicating the retention ratio of the current input information, $\tilde{C}_t$ is the candidate cell state, reflecting the candidate values of new information, W_i and W_c are the weight matrix for both the input gate and the candidate cell state, while b_c is their respective bias terms.

Finally, the output gate integrates the above information to obtain the output signal h_t with the following equation:

$$o_t = \sigma(W_o \cdot [h_{t-1}, x_t] + b_0) \tag{7}$$

$$h_t = \tanh(C_t) * o_t \tag{8}$$

where σ represents the sigmod neural network layer, and W_o and b_o represent the weight matrix and deviation vector. Through their action, the LSTM network is able to realize the weighting of input data and the updating of the memory state to better capture the dependencies in the sequence data[44].

Despite the improvement of LSTM, the forgetting mechanism exhibits exponential decay of information limiting its ability to capture long time scale information. In contrast, the TCN specific dilation causal convolution and residual connection can adjust the sensory field size by the number of layers, dilation factor, and filter size,

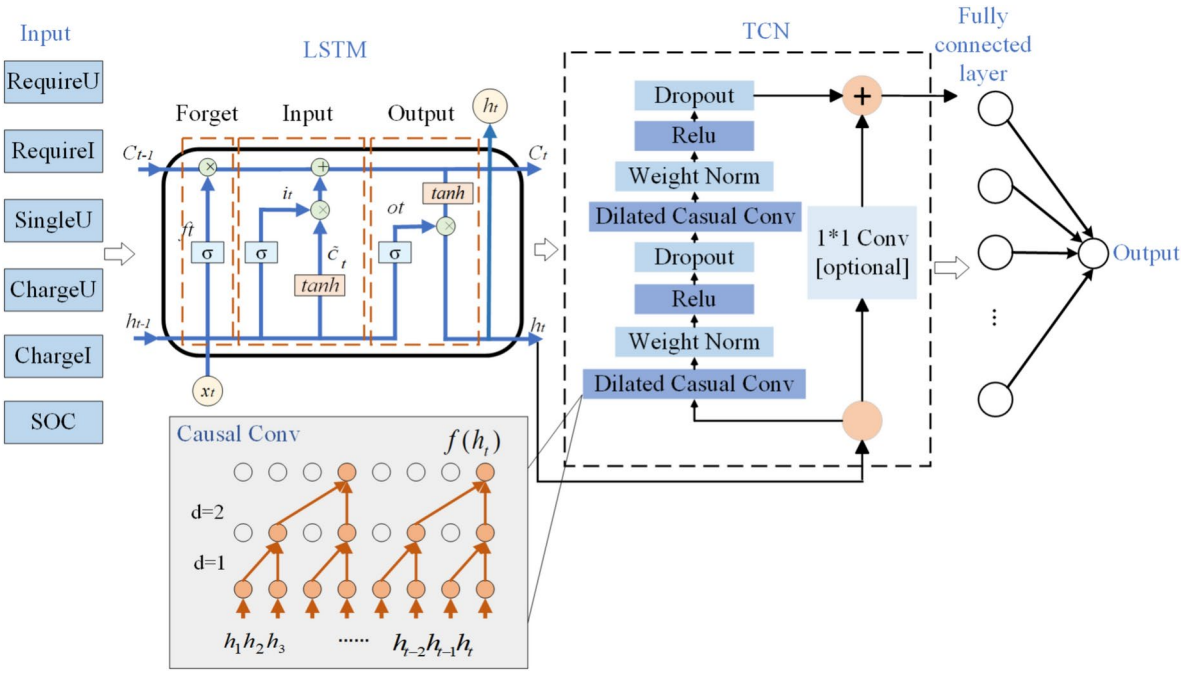

Fig. 3. LSTM-TCN model.

which enables the model to obtain stable results even when dealing with long-time input data[45]such as EV charging.

Therefore, the LSTM network output is used as an input to the TCN network. In this case, the predicted output temperature y_t of the TCN network has to be determined by the inputs prior to the moment t. To achieve this goal, the initial layer of the TCN uses a one-dimensional dilated causal convolution (shown in Fig. 3), which takes the output of the LSTM network layer as input. In each intermediate layer, the size of the input layer is kept constant and zero padding is used to obtain the same size of the subsequent layer as the previous one[46]. In each layer, a convolution operation is performed to extract features between the charging data and the charging temperature. The computational formula is given below:

$$f(h_t) = \sum_{k=1}^{L} w_k \cdot h_{t-d \cdot k} \tag{9}$$

where h_t is the input sequence and L is the kernel size, w_k is the kernel weights, and d is the dilation rate.

However, the traditional convolution operation is a purely linear operation involving only addition and multiplication of matrices. Considering the complexity and nonlinear characteristics of EV charging data, this model introduces nonlinear units (ReLU) for nonlinear adjustment[47].

Finally, in order to endow the network with the capability of cross-layer information propagation and ensure consistency between input and output, the causal convolutional component is connected to the one-dimensional convolutional network through residual connections, as indicated by the plus sign in the Fig. 3, resulting in the temperature prediction output. The output equation can be expressed as follows:

$$y_t = R[f(h_t) + Conv1D(h_t)] \tag{10}$$

where $f(h_t)$ is dilated convolution operation, R represents the ReLU activation function, and $Conv1D(h_t)$ is the one-dimensional convolution operation.

To summarize, this paper adopts the LSTM network to extract sequence features and feeds these features into the TCN network to establish a predictive model for the temperature of EV lithium-ion battery during charging. By doing so, we obtain highly efficient and accurate predictions.

Model evaluation and validation standards

The evaluation metrics selected for the neural networks include three commonly used indicators: Mean Absolute Error (*MAE*), Root Mean Squared Error (*RMSE*), and Coefficient of Determination (R Squared, R^2)[48,49]. The specific formulas are as follows:

$$MAE = \frac{1}{n} \sum_{t=1}^{n} |y_t - \hat{y}_t| \tag{11}$$

$$RMSE = \sqrt{\frac{1}{n} \sum\nolimits_{t=1}^{n} (y_t - \hat{y}_t)^2} \tag{12}$$

$$R2 = 1 - \frac{D_{res}}{D_{tot}} = 1 - \frac{\sum_{t=1}^{n} (\hat{y}_t - y_t)^2}{\sum_{t=1}^{n} (\bar{y}_t - y_t)^2} \tag{13}$$

where y_t represents the true values of EV charging temperature, $\hat{y}_t$ represents the predicted values of EV charging temperature, D_{res} represents the sum of squared residuals, D_{tot} represents the sum of squared deviations, and $\bar{y}_i$ represents the average output charging temperature. Smaller values of *MAE* and *RMSE* indicate higher accuracy of the model, while R^2 ranges from 0 to 1, with values closer to 1 indicating a higher degree of model fit. These definitions are essential for evaluating the performance of the proposed model in predicting EV charging temperature.

Design of thermal runaway warning discrimination

The sliding window technique is primarily applied in the processing and analysis of time series data. By moving a fixed-sized window across the entire dataset, it enables segmenting the lithium-ion battery charging time series data. This allows for capturing key features such as trends, periodicity, and anomalies in the time series data, while minimizing the impact of erroneous data[50]. The process of the sliding window technique is illustrated in Fig. 4.

The residual analysis technique is primarily employed to identify system anomalies or potential faults by monitoring the differences between actual observed values and model predicted values[51]. As temperature values do not exhibit clear trends over short periods of time, analyzing charging temperature using residual calculations can more effectively capture abnormal changes.

Take the sliding window with length N, calculate the mean residual value and the standard deviation of the residual between the current temperature and the temperature in the sliding window, and the formula is as follows:

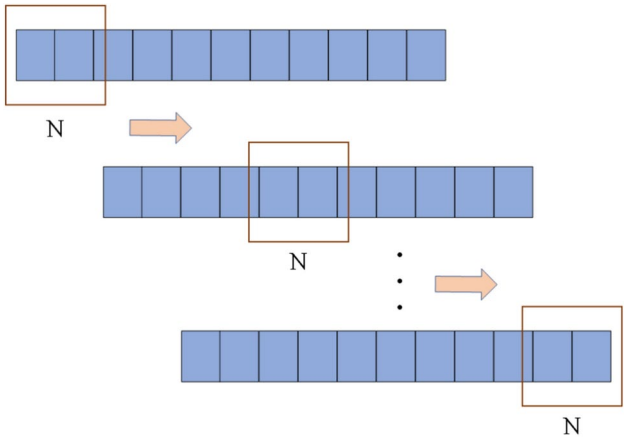

Fig. 4. Sliding window process.

$$\begin{cases} \bar{X} = \frac{1}{N}\sum_{t=1}^{n} e_t \\ S = \sqrt{\frac{1}{N-1}\sum_{t=1}^{n}\left(e_t - \bar{X}\right)} \end{cases} \tag{14}$$

where $\bar{X}$ is the mean residual value, e_t is the residual value of the sliding window at time t, and S is the standard deviation of the residuals.

After calculating the residuals of the normal charging data of the lithium battery of electric vehicles, the mean value of the maximum residual and the standard deviation of the residuals are obtained, and the pre-alarm threshold is calculated. The formula is as follows:

$$\begin{cases} \pm X_{\mathrm{E}} = \pm\mu_1 \bar{X}_{\max} \\ S_{\mathrm{E}} = \mu_2 S_{\max} \end{cases} \tag{15}$$

where μ_1 and μ_2 are the early warning coefficients, which are usually integers obtained based on experience, $\pm X_{\mathrm{E}}$ is the upper and lower limits of the mean threshold of the pre-alarm residuals, and S_{E} is the upper limit of the standard deviation of the pre-alarm residuals.

Design of thermal runaway warning discrimination

In this paper, the thermal runaway prediction and safety warning methods of lithium battery charging temperature for electric vehicles are combined, as shown in Fig. 5. Firstly, the charging parameters of lithium batteries are obtained by the charging network BMS system[52]. The charging pile and the electric vehicles use the international standard CAN communication protocol for data transmission, and the collected real-time data is preprocessed such as outlier elimination, missing value completion and normalization to obtain the time series data required for feature extraction.

Then, the LSTM-TCN temperature prediction model is designed, the time series data was input into the model training, and the structure and parameters of the model are adjusted by analyzing the prediction results, and finally the temperature prediction model with the highest accuracy is obtained. The algorithm structure is shown in Algorithm 1.

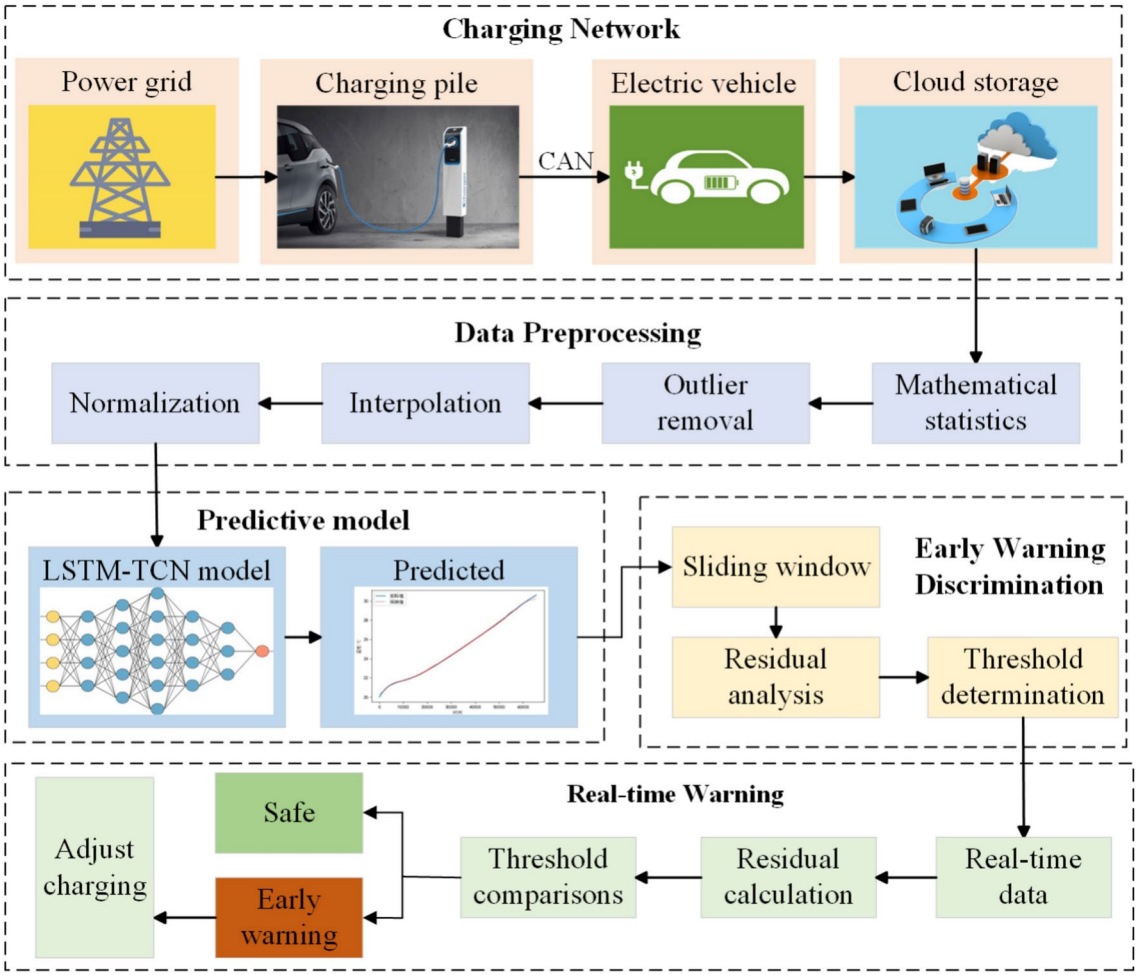

Fig. 5. Early warning process of thermal runaway of lithium battery in electric vehicles.

Input: time series $\{x_1, x_2, \ldots, x_{t-1}, x_t\}$
for LSTM layers $a = 1 : 2$ **do**
  for neuron number $i = 1 : 60$ **do**
    information discarded (Eq.(4))
    information retention (Eq.(5)(6))
    information output (Eq.(7)(8))
  end for
end for
for TCN dilation-rate $= 1 : 2$ **do**
  dilated causal conv (Eq.(6))
  weight norm
  ReLU
end for
Connection with 1D Conv residuals
return predicted $T\{y_1, y_2, \ldots, y_{t-1}, y_t\}$

Algorithm 1. Integration of LSTM-TCN

Then, the sliding window method is used to analyze the residuals of the normal charging data of different types of EV lithium-ion batteries, determine the temperature warning threshold, and carry out dynamic early warning. Figure 6 shows the early warning process. After processing the predicted temperature with a fixed-length sliding window, the standard deviation of the residuals and the mean of the residuals are calculated.

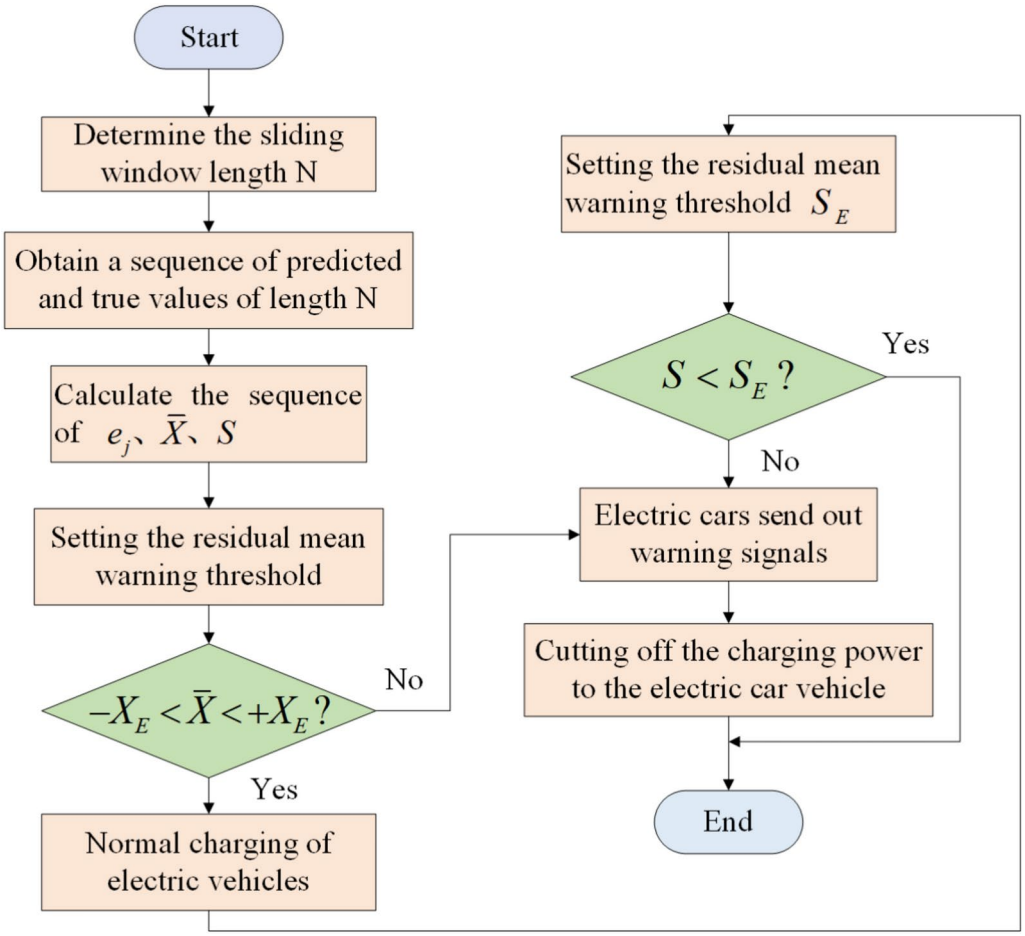

Fig. 6. Sliding window and residual analysis process.

According to Eq. (15), the early warning threshold is established. The residual standard deviation between the real-time predicted value and the actual value of the EV lithium-ion battery charging data is then compared with the mean residual value and the threshold. When the mean residual or residual standard deviation of the real-time charging data exceeds the limit, the charging device issues a thermal runaway warning. It also takes protective measures to ensure the safety of the vehicle and personnel.

Finally, the thermal runaway and normal data of different types of lithium battery charging for electric vehicles are used for experimental verification to further determine the accuracy and feasibility of the method.

Experimental verification and analysis

Experiment preparation and subject selection

In this experiment, 12th Gen Intel(R) Core(TM) i5-12500H @3.10 GHz was used as the processor, Python 3.8 and TensorFlow 2.4.1 were used for programming, and the Keras framework was used to build a deep learning model.

The EV charging network is an EV charging facility management system based on the Internet and Internet of Things technology, which provides convenient charging services for EV by connecting various charging piles, charging stations, EVs and related cloud platforms. In this experiment, the relevant periodic data were collected through the EV charging network as the dataset of this experiment.

In this experiment, to achieve the most accurate predictive results, we selected *MAE* and *RMSE* for Nickel manganese cobalt battery (NMC) and Lithium Iron phosphate battery (LFP) as evaluation metrics. The model parameters were adjusted by comparing the errors of LSTM and TCN under different parameter settings. The specific accuracy metrics are presented in Tables 4 and 5.

The final model configuration selected includes an LSTM with 3 hidden layers and 90 neurons. For the TCN, the maximum dilation factor is set to 4, with 20 filters.

Taking two types of EV lithium-ion batteries, namely, NMC and LFP, as the experimental objects. The power battery capacity of the NMC is 91.5Ah, while the power battery capacity of the LFP is 207Ah. To demonstrate the universality of this method, normal charging data from the two types of electric vehicles at a normal room temperature of 25°C were used for model training. Then, abnormal charging data from the two types of electric vehicles under low temperature (−15°C) and high temperature (40°C) conditions were utilized to validate the method.

	Number of implied layers							
	MAE				*RMSE*			
Number of neurons	1	2	3	4	1	2	3	4
30	0.035	0.029	0.081	0.034	0.029	0.032	0.912	0.081
60	0.049	0.041	0.030	0.037	0.034	0.053	0.035	0.043
90	0.037	0.029	0.035	0.031	0.036	0.045	0.023	0.041

Table 4. Results of *MAE* and *RMSE* with different parameters of LSTM.

	Number of max dilation rate							
	MAE				*RMSE*			
Number of filters	1	2	4	8	1	2	4	8
10	0.065	0.051	0.044	0.037	0.061	0.051	0.063	0.091
20	0.037	0.045	0.031	0.035	0.074	0.054	0.049	0.049
30	0.047	0.061	0.037	0.084	0.071	0.052	0.093	0.051

Table 5. Results of *MAE* and *RMSE* with different parameters of TCN.

	NMC			LFP		
Model type	*MAE*	*RMSE*	R^2	*MAE*	*RMSE*	R^2
LSTM-TCN	0.009	0.012	0.99	0.027	0.037	0.99
TCN-LSTM	0.023	0.027	0.99	0.072	0.096	0.99
CNN-LSTM	0.019	0.033	0.99	0.066	0.087	0.99
CNN-TCN	0.024	0.031	0.98	0.085	0.107	0.98
LSTM	0.029	0.023	0.98	0.081	0.112	0.97
TCN	0.031	0.049	0.98	0.084	0.126	0.97
CNN	0.038	0.048	0.98	0.121	0.139	0.97

Table 6. Multi-model prediction accuracy.

Model comparison and analysis

In the process of thermal runaway of EV lithium-ion battery, the abnormal increase in battery temperature is one of the main characteristics. Therefore, accurate prediction of charging temperature can detect abnormal temperature increases in advance, which can help to take timely measures to avoid potential thermal runaway. At the same time, using multiple parameters as inputs can make the deep learning Xi model map to more complex features and relationships, and improve the sensitivity of the model to potential risks.

Both the LSTM network and the TCN network exhibit strong processing capabilities for time series data. Therefore, the normal charging data of two different types of electric vehicle lithium batteries at 25°C are used as input for the LSTM-TCN model and the TCN-LSTM model. The prediction results show that the evaluation indexes of the LSTM-TCN model for the two types of electric vehicle lithium batteries are higher than those of the TCN-LSTM model. The specific values are presented in the model evaluation data in Table 6. At the same time, it is shown that for the charging data of EV lithium-ion battery, the short-term time series features are extracted first, and then the long-term features are summarized, and more accurate prediction results can be obtained, as shown in Fig. 7.

To verify the wide accuracy of LSTM-TCN, we compared it with other models such as CNN-LSTM, CNN-TCN, LSTM, TCN, and CNN using the same charging dataset. As shown in the multiple-model temperature prediction results comparison chart in Fig. 8, during the three charging periods, the LSTM-TCN model had a good fitting effect, while the other models were more likely to produce prediction deviations due to insufficient data points in the later stage. Meanwhile, for the evaluation indicators of the LSTM-TCN model, *MAE* was 0.009, *RMSE* was 0.012, and R^2 was 0.99 for NMC battery, and *MAE* was 0.026, *RMSE* was 0.036, and R^2 was 0.99 for LFP battery, all of which were superior to the other models. Specific evaluation indicator data are shown in Table 6.

In summary, we selected the LSTM-TCN model as the temperature prediction model in this paper, providing a data foundation for alarm threshold setting and method practicality verification.

Early warning analysis and verification

We selected a sliding window length of N=100 and determined the warning threshold by training and residual analysis of normal charging data at 25°C. Abnormal charging data from two types of electric vehicle lithium

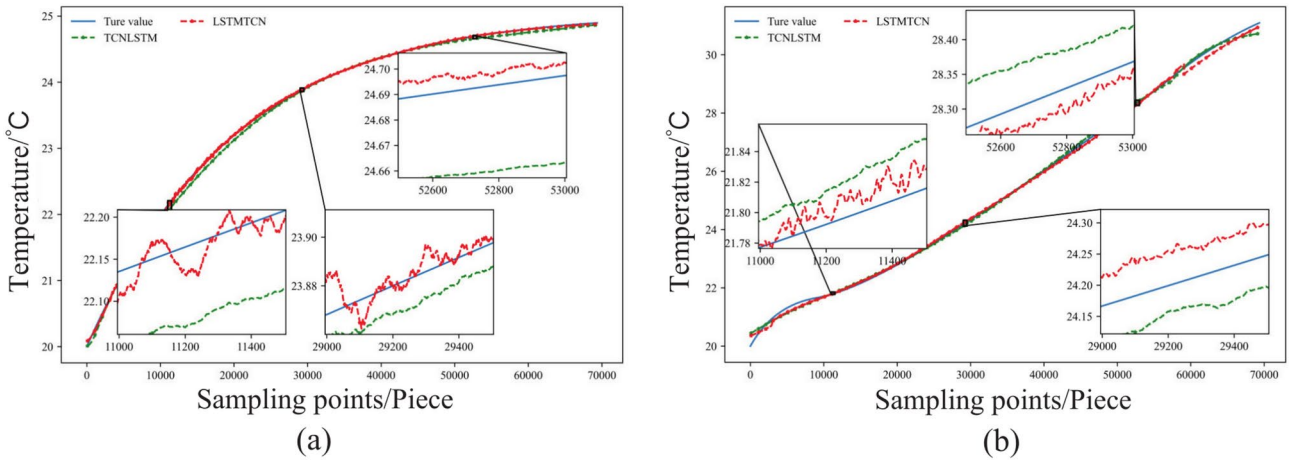

Fig. 7. Prediction plots of normal charging temperature for both models.

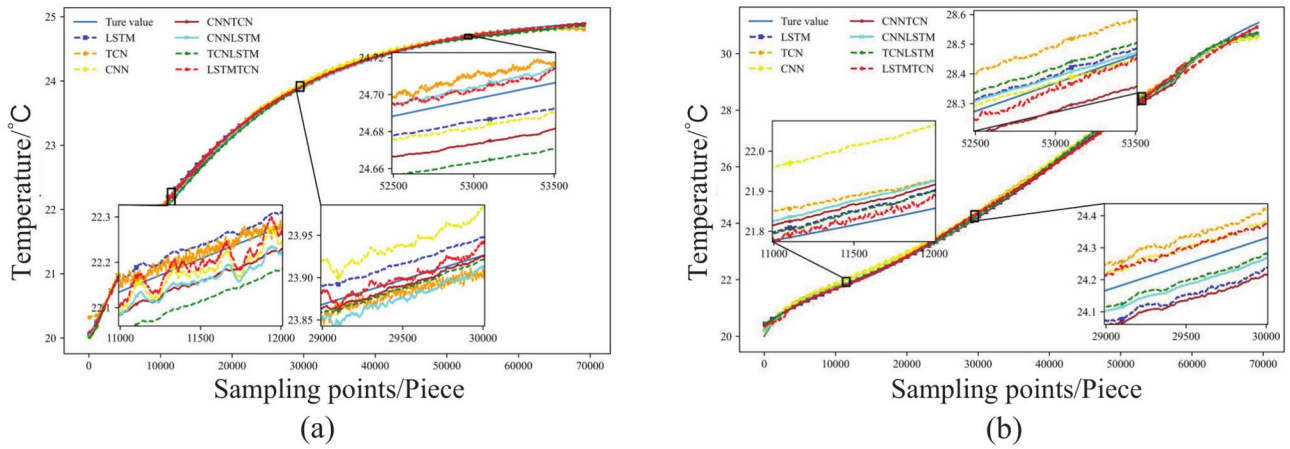

Fig. 8. Prediction plots of normal charging temperature for multiple models.

batteries were selected for pre-alarm experiments to determine the practicality and accuracy of the thermal runaway warning model.

According to Eq. (14), the residual standard deviation and mean of normal charging states for the two types of lithium batteries were calculated, as shown in Figs. 9 and 10. For the NMC battery, the maximum value of residual standard deviation 0.026, and the maximum absolute value of residual mean is 0.063. For the LFP battery, the maximum value of residual standard deviation is 0.206, and the maximum absolute value of residual mean is 0.011. Using Eq. (15), the thermal runaway pre-alarm thresholds are calculated, with μ_1 selected as 2 and μ_2 as 4.5. The pre-alarm threshold for NMC residual standard deviation is calculated as 0.052, and the pre-alarm threshold for residual mean is 0.284. The pre-alarm threshold for LFP residual standard deviation is 0.041, and the pre-alarm threshold for residual mean is 0.481.

Due to the significant impact of extreme environmental temperatures on thermal runaway during charging of EV lithium-ion batteries, the charging data under low temperature and high temperature conditions for NMC and LFP batteries are selected as input for the trained predictive model. The predicted results are then analyzed through residual analysis by comparing them with the actual values. Based on the analysis results, the pre-alarm moments are determined and compared with the actual thermal runaway moments.

For the selected abnormal sample data of the NMC battery at − 15 °C, the actual thermal runaway moment is observed at the 58183th sampling point. As shown in Fig. 11, the pre-alarm moment for residual standard deviation of the warning model is at the 57624th sampling point, which is 559 sampling points or 27.95 s ahead of the actual event. On the other hand, the pre-alarm moment for the residual mean is at the 57638th sampling point, 555 sampling points or 27.75 s ahead of the actual event.

For the selected abnormal sample data of the LFP battery at − 15 °C, the actual thermal runaway moment is observed at the 58246th sampling point. As shown in Fig. 12, the pre-alarm moment for residual standard deviation of the warning model is at the 57713th sampling point, which is 533 sampling points or 26.65 s ahead of the actual event. On the other hand, the pre-alarm moment for the residual mean is at the 57696th sampling point, 550 sampling points or 27.50 s ahead of the actual event.

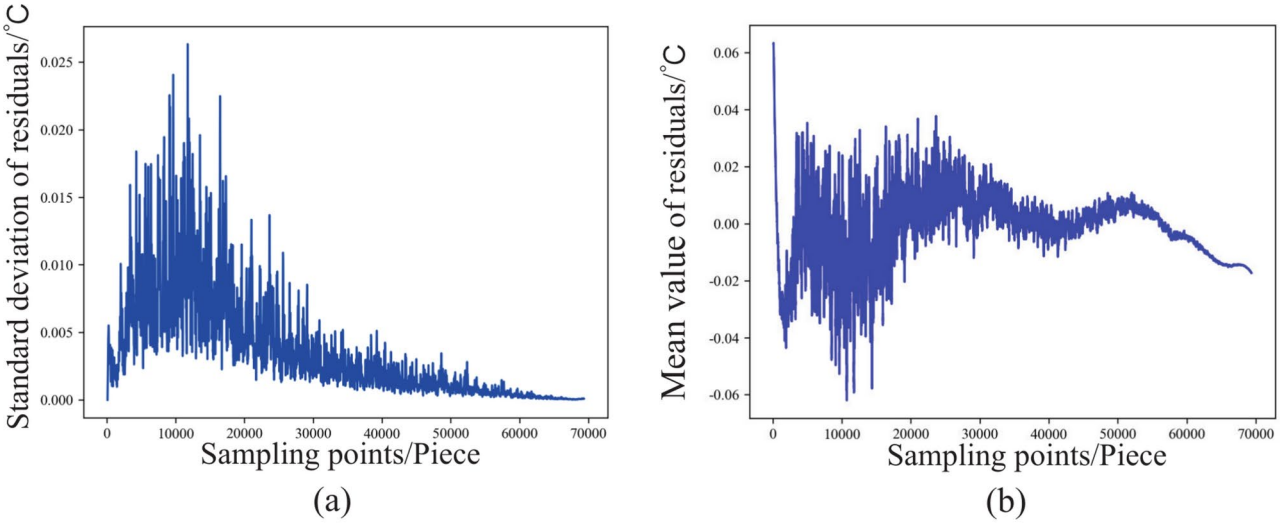

Fig. 9. NMC normal charge residual analysis.

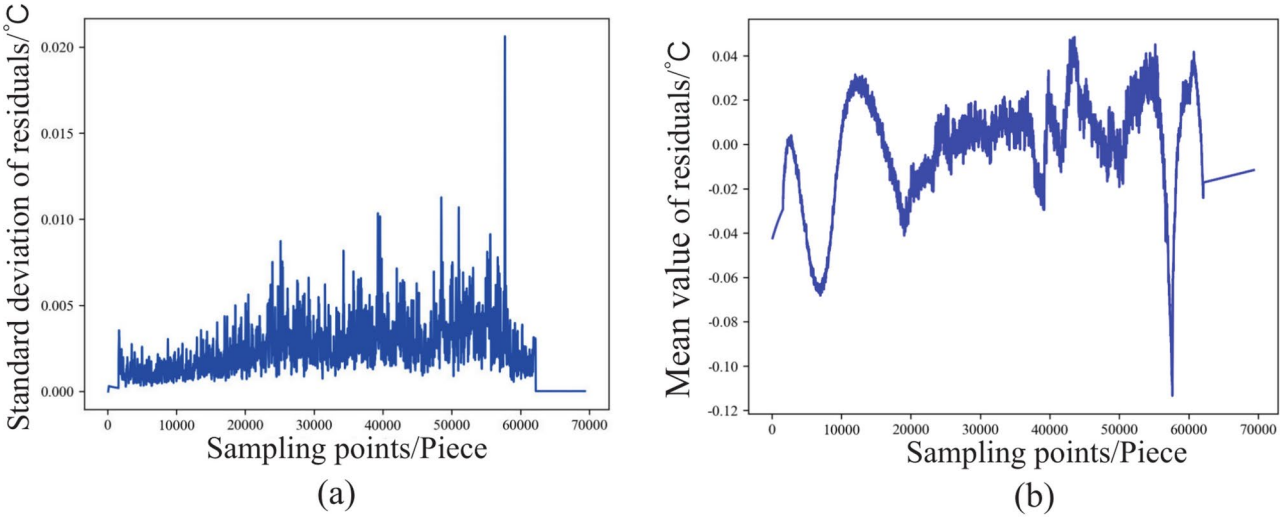

Fig. 10. LFP normal charge residual analysis.

For the selected abnormal sample data of the NMC battery at 35 °C, the actual thermal runaway moment is observed at the 58096th sampling point. As shown in Fig. 13, the pre-alarm moment for residual standard deviation of the warning model is at the 57656th sampling point, which is 440 sampling points or 22.00 s ahead of the actual event. On the other hand, the pre-alarm moment for the residual mean is at the 57680th sampling point, 416 sampling points or 20.80 s ahead of the actual event.

For the selected abnormal sample data of the LFP battery at 35 °C, the actual thermal runaway moment is observed at the 50884th sampling point. As shown in Fig. 14, the pre-alarm moment for residual standard deviation of the warning model is at the 50600th sampling point, which is 284 sampling points or 14.20 s ahead of the actual event. On the other hand, the pre-alarm moment for the residual mean is at the 50685th sampling point, 199 sampling points or 9.95 s ahead of the actual event.

Based on the experimental results, it is known that it is more difficult to issue warnings for lithium-ion batteries in electric vehicles when the ambient temperature is high. The shortest warning time is 9.95 s, which is sufficient to adjust the charging method to prevent thermal runaway events from occurring.

In conclusion, under conditions of excessively high or low ambient temperatures, utilizing residual analysis to issue warnings based on the predicted charging temperature values of lithium-ion batteries allows sufficient time for adjusting the charging method of electric vehicles, thereby ensuring the safety of both the individuals and the vehicles.

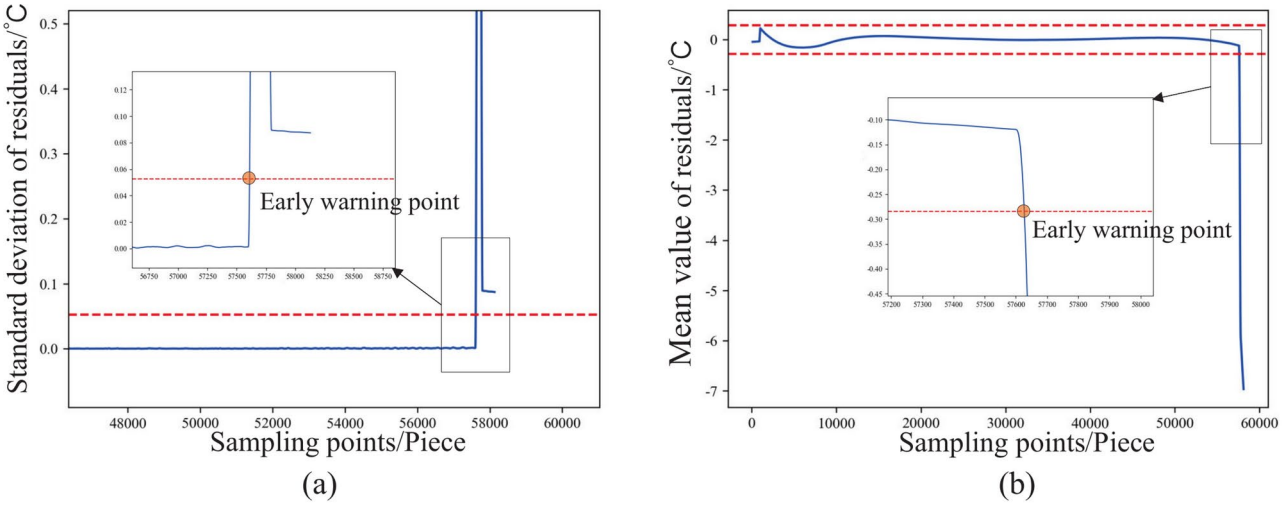

Fig. 11. Thermal runaway data early warning analysis of NMC charging at -15°C.

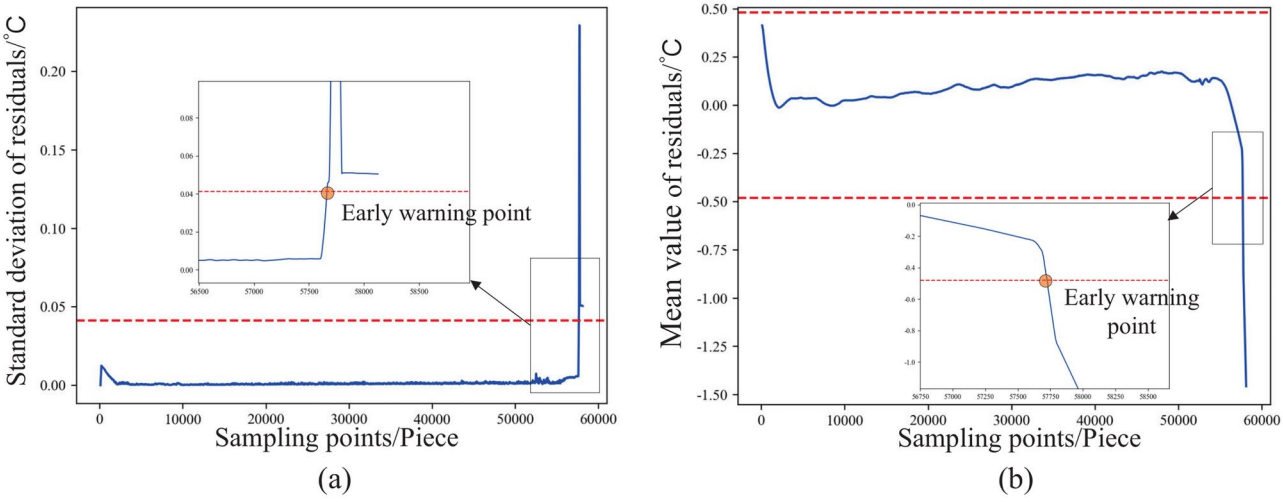

Fig. 12. Thermal runaway data early warning analysis of FPL charging at -15°C.

Conclusion

In order to address the safety concerns posed by thermal runaway events in EV lithium-ion battery during the charging process, this paper proposed a charging thermal runaway warning method based on the charging network for EV lithium-ion battery. Using the LSTM-TCN model for charging temperature prediction, experimental results demonstrate that this model reduces *MAE* values by up to 9.4% and *RMSE* by up to 10.2% compared to other models, with R^2 consistently reaching 99.9%. The residual analysis-based warning system showed effective early warning times ranging from a minimum of 9.95 s to a maximum of 22.00 s across thermal runaway tests conducted on NMC and LFP Lithium-ion batteries in EVs under different temperatures. This approach enables proactive warning before thermal runaway initiation, enhancing safety for both vehicle occupants and the vehicle itself.

Although our method has made contributions in the field of charging safety for EV lithium-ion battery, there are certain limitations that should be acknowledged:

(1) Insufficient research on charging methods for EV lithium-ion battery may result in suboptimal model training. Future studies will explore different charging configurations to enhance the effectiveness of the approach.
(2) The availability of high-quality historical data is limited, which restricts the wide-ranging investigation of various vehicle models. Collecting more diverse charging data from different types of EV lithium-ion batteries will improve the generalizability of this method in future work.

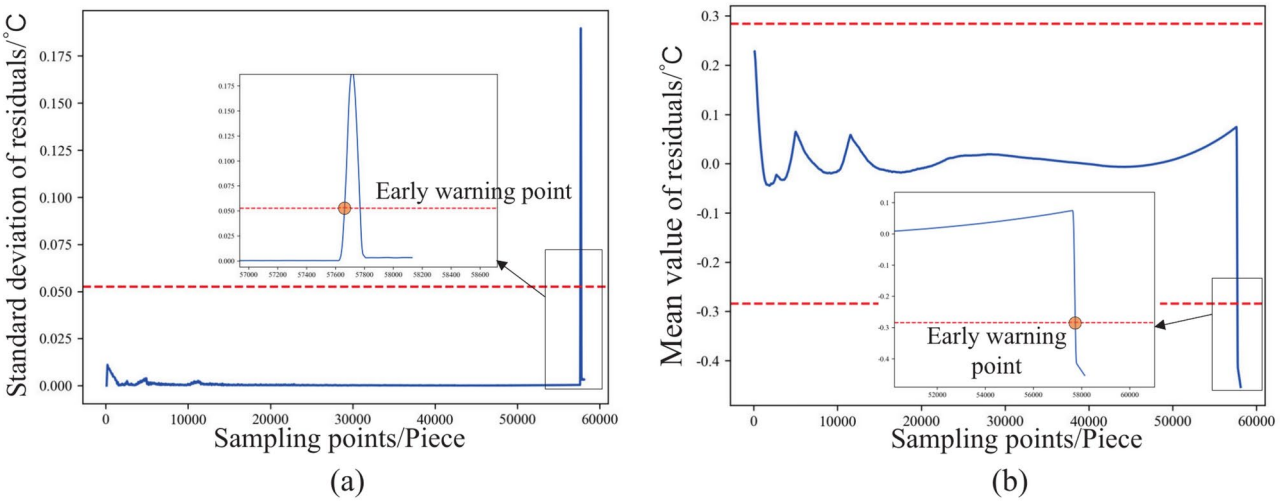

Fig. 13. Thermal runaway data early warning analysis of NMC charging at 35°C.

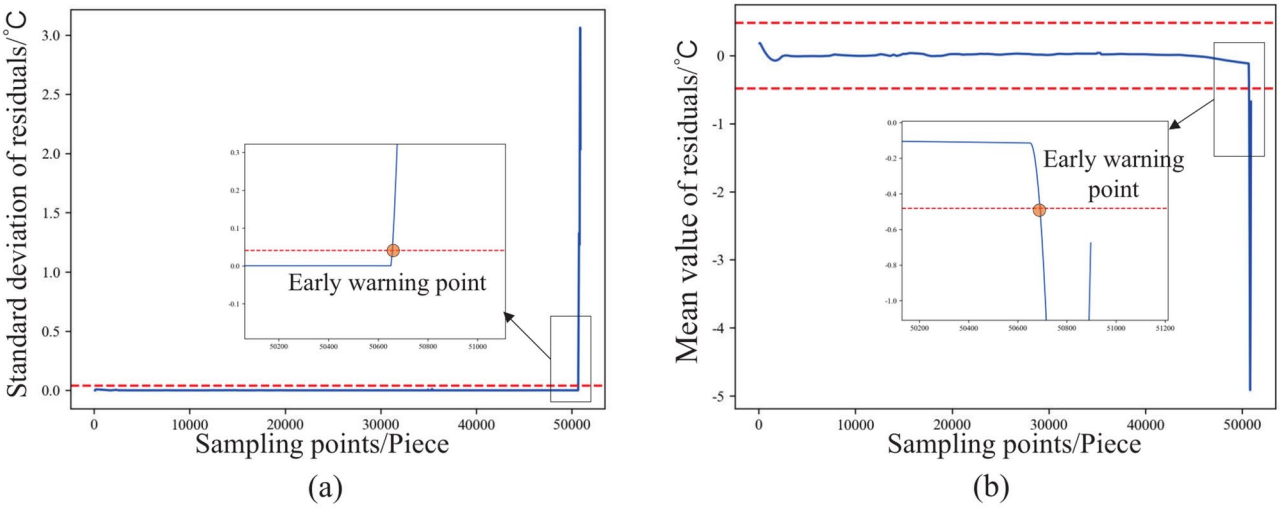

Fig. 14. Thermal runaway data early warning analysis of FPL charging at 35°C.

Data availability

Due to the lack of publicly available datasets for this study, the datasets used during the current study period can be obtained from the corresponding authors upon reasonable request.

Received: 24 September 2024; Accepted: 3 March 2025
Published online: 06 March 2025

References

1. Duan, J. et al. Building safe lithium-ion batteries for electric vehicles: A review. *Electrochem Energy R.* **3**, 1–42. https://doi.org/10.1007/s41918-019-00060-4 (2022).
2. Zhang, X. et al. A review on thermal management of lithium-ion batteries for electric vehicles. *Energy* **238**, 121652. https://doi.org/10.1016/j.energy.2021.121652 (2022).
3. Zhang, Q. et al. Research on the lower explosion limit of thermal runaway gas in lithium batteries under high-temperature and slight overcharge conditions. *J. Energy Storage* **79**, 109976. https://doi.org/10.1016/j.est.2023.109976 (2024).
4. Feng, X. et al. Thermal runaway mechanism of lithium ion battery for electric vehicles: A review. *Energy Storage Mater.* **10**, 246–267. https://doi.org/10.1016/j.ensm.2017.05.013 (2018).
5. He, D. et al. Research advances on thermal runaway mechanism of lithium-ion batteries and safety improvement. *Sustain. Mater. Technol.* **41**, e01017. https://doi.org/10.1016/j.susmat.2024.e01017 (2024).
6. Du, J., Azuaje-Berbecí, B. & Ertan, H. A model for the prediction of thermal runaway in lithium-ion batteries. *J. Energy Storage* **90**, 111831. https://doi.org/10.1016/j.est.2024.111831 (2024).
7. Wassiliadis, N. et al. Review of fast charging strategies for lithium-ion battery systems and their applicability for battery electric vehicles. *J. Energy Storage* **44**, 103306. https://doi.org/10.1016/j.est.2021.103306 (2021).

8. Khan, A. et al. A state-of-the-art review on heating and cooling of lithium-ion batteries for electric vehicles. *J. Energy Storage* **76**, 109852. https://doi.org/10.1016/j.est.2023.109852 (2023).
9. Jia, Q. et al. A comprehensive review on thermal runaway model of a lithium-ion battery: Mechanism, thermal, mechanical, propagation, gas venting and combustion. *Renew. Energy* **229**, 120762. https://doi.org/10.1016/j.renene.2024.120762 (2024).
10. Liu, B. et al. Reducing lithium-ion battery thermal runaway risk based on an integrated cooling strategy for electric vehicles. *Int. J. Heat Mass Transf.* **216**, 124594. https://doi.org/10.1016/j.ijheatmasstransfer.2023.124594 (2023).
11. Jiang, L. et al. Data-driven fault diagnosis and thermal runaway warning for battery packs using real-world vehicle data. *Energy* **234**, 121266. https://doi.org/10.1016/j.energy.2021.121266 (2021).
12. Song, Y. et al. Electric-controlled pressure relief valve for enhanced safety in liquid-cooled lithium-ion battery packs. *J. Energy Chem.* **90**, 98–109. https://doi.org/10.1016/j.jechem.2023.11.007 (2024).
13. Hu, X. et al. Advancements in the safety of lithium-ion battery: The trigger, consequence and mitigation method of thermal runaway. *Chem. Eng. J.* **481**, 148450. https://doi.org/10.1016/j.cej.2023.148450 (2024).
14. Bi, S. et al. Understanding the combustion characteristics and establishing a safety evaluation technique based on the overcharged thermal runaway of lithium-ion batteries. *J. Energy Storage* **73**, 109039. https://doi.org/10.1016/j.est.2023.109039 (2023).
15. Zhao, R., Gu, J. & Liu, J. Optimization of a phase change material based internal cooling system for cylindrical Li-ion battery pack and a hybrid cooling design. *Energy* **135**, 811–822. https://doi.org/10.1016/j.energy.2017.06.168 (2017).
16. Ni, R. et al. Prevention and suppression effects of phase change material on thermal runaway in batteries. *Case Stud. Therm. Eng.* **48**, 103160. https://doi.org/10.1016/j.csite.2023.103160 (2023).
17. Drees, R., Lienesch, F. & Kurrat, M. Fast charging lithium-ion battery formation based on simulations with an electrode equivalent circuit model. *J. Energy Storage* **36**, 102345. https://doi.org/10.1016/j.est.2021.102345 (2021).
18. Munonde, T. S. & Raphulu, M. C. Review on titanium dioxide nanostructured electrode materials for high-performance lithium batteries. *J. Energy Storage* **78**, 110064. https://doi.org/10.1016/j.est.2023.110064 (2024).
19. Xu, J. et al. Prevent thermal runaway of lithium-ion batteries with minichannel cooling. *Appl. Therm. Eng.* **110**, 883–890. https://doi.org/10.1016/j.applthermaleng.2016.08.151 (2017).
20. Hu, D. et al. A review on thermal runaway warning technology for lithium-ion batteries. *Renew. Sustain. Energy Rev.* **206**, 114882. https://doi.org/10.1016/j.rser.2024.114882 (2024).
21. Kong, D., Lv, H., Ping, P. & Wang, G. A review of early warning methods of thermal runaway of lithium ion batteries. *J. Energy Storage* **64**, 107073. https://doi.org/10.1016/j.est.2023.107073 (2023).
22. Nie, B., Dong, Y. & Chang, L. The evolution of thermal runaway parameters of lithium-ion batteries under different abuse conditions: A review. *J. Energy Storage* **96**, 112624. https://doi.org/10.1016/j.est.2024.112624 (2024).
23. Goswami, B. et al. A combined multiphysics modeling and deep learning framework to predict thermal runaway in cylindrical Li-ion batteries. *J. Power Sources* **595**, 234065. https://doi.org/10.1016/j.jpowsour.2024.234065 (2024).
24. Zheng, X. et al. An early warning protection method for electric vehicle charging based on the hybrid neural network model. *World Electr . Veh. J.* **13**(7), 128–128. https://doi.org/10.3390/WEVJ13070128 (2022).
25. Hou, Q. et al. A vehicle alarm network for high-temperature fault diagnosis of electric vehicles. *Appl. Intell.* **53**(6), 6230–6247. https://doi.org/10.1007/S10489-022-03615-Z (2023).
26. Yang, Y. et al. Towards a safer lithium-ion batteries: A critical review on cause, characteristics, warning and disposal strategy for thermal runaway. *Adv. Appl. Energy* **11**, 100146. https://doi.org/10.1016/j.adapen.2023.100146 (2023).
27. Zhang, Y. et al. Numerical modeling on thermal runaway triggered by local overheating for lithium iron phosphate battery. *Appl. Therm. Eng.* **192**, 116928. https://doi.org/10.1016/j.applthermaleng.2021.116928 (2021).
28. Mallick, S. & Gayen, D. Thermal behaviour and thermal runaway propagation in lithium-ion battery systems-A critical review. *J. Energy Storage* **192**, 106894. https://doi.org/10.1016/j.est.2023.106894 (2023).
29. Kong, L. et al. Strategies to solve lithium battery thermal runaway: From mechanism to modification. *Electrochem. Energy R.* **4**, 633–679. https://doi.org/10.1007/s41918-021-00109-3 (2021).
30. Ren, D. et al. Investigating the relationship between internal short circuit and thermal runaway of lithium-ion batteries under thermal abuse condition. *Energy Storage Mater.* **34**, 563–573. https://doi.org/10.1016/j.ensm.2020.10.020 (2021).
31. Mallick, S. & Gayen, D. Thermal behaviour and thermal runaway propagation in lithium-ion battery systems-A critical review. *J. Energy Storage* **62**, 106894. https://doi.org/10.1016/j.est.2023.106894 (2023).
32. Peng, R. et al. Thermal runaway modeling of lithium-ion batteries at different scales: Recent advances and perspectives. *Energy Storage Mater.* **69**, 103417. https://doi.org/10.1016/j.ensm.2024.103417 (2024).
33. Shan, T. et al. Insights into extreme thermal runaway scenarios of lithium-ion batteries fire and explosion: A critical review. *J. Energy Storage* **88**, 111532. https://doi.org/10.1016/j.est.2024.111532 (2024).
34. Wang, H. et al. Dynamic thermophysical modeling of thermal runaway propagation and parametric sensitivity analysis for large format lithium-ion battery modules. *J. Power Sources* **520**, 230724. https://doi.org/10.1016/j.jpowsour.2021.230724 (2022).
35. Gai, Q. et al. An in-situ bicomponent polymeric matrix solid electrolyte for solid-state Lithium metal batteries with extended cycling-life. *J. Energy Storage* **80**, 110150. https://doi.org/10.1016/J.EST.2023.110150 (2024).
36. Xiao, Y. et al. Review of mechanical abuse related thermal runaway models of lithium-ion batteries at different scales. *J. Energy Storage* **64**, 107145. https://doi.org/10.1016/j.est.2023.107145 (2024).
37. Hong, J. et al. Investigation on overcharge-caused thermal runaway of lithium-ion batteries in real-world electric vehicles. *Appl. Energy* **321**, 119229. https://doi.org/10.1016/j.apenergy.2022.119229 (2022).
38. Jiang, L. et al. Data-driven fault diagnosis and thermal runaway warning for battery packs using real-world vehicle data. *Energy* **234**, 121266. https://doi.org/10.1016/j.energy.2021.121266 (2021).
39. Gao, D. et al. Novel semi-supervised fault diagnosis method combining Tri-training and Deep belief network for charging equipment of electric vehicle. *Int. J. Automot. Technol.* **23**, 1727–1737. https://doi.org/10.1007/s12239-022-0150-7 (2022).
40. Kiran Kumar, V., Ramesh, K. V. & Rakesh, V. Optimizing LSTM and Bi-LSTM models for crop yield prediction and comparison of their performance with traditional machine learning techniques. *Appl. Intell.* **53**(23), 28291–28309. https://doi.org/10.1007/S10489-023-05005-5 (2023).
41. Zhang, S., Huang, P. & Yan, W. A data-driven approach for railway in-train forces monitoring. *Adv. Eng. Inform.* **59**, 102258. https://doi.org/10.1016/j.aei.2023.102258 (2024).
42. Wang, X., Bai, Y. & Liu, X. Prediction of railroad track geometry change using a hybrid CNN-LSTM spatial-temporal model. *Adv. Eng. Inform.* **58**, 102235. https://doi.org/10.1016/j.aei.2023.102235 (2023).
43. Li, B., Lv, X. & Chen, J. Demand and supply gap analysis of Chinese new energy vehicle charging infrastructure: Based on CNN-LSTM prediction model. *Renew. Energy* **220**, 119618. https://doi.org/10.1016/j.renene.2023.119618 (2024).
44. Ma, S. et al. TCLN: A Transformer-based Conv-LSTM network for multivariate time series forecasting. *Appl. Intell.* **53**(23), 28401–28417. https://doi.org/10.1007/S10489-023-04980-Z (2023).
45. Li, F. et al. State-of-charge estimation of lithium-ion battery based on second order resistor-capacitance circuit-PSO-TCN model. *Energy* **289**, 130025. https://doi.org/10.1016/j.energy.2023.130025 (2023).
46. Wang, Z. et al. Cluster-based industrial KPIs forecasting considering the periodicity and holiday effect using LSTM network and MSVR. *Adv. Eng. Inform.* **56**, 101916. https://doi.org/10.1016/j.aei.2023.101916 (2023).
47. Zhang, T. et al. A hybrid electric vehicle load classification and forecasting approach based on GBDT algorithm and temporal convolutional network. *Appl. Energy* **351**, 121768. https://doi.org/10.1016/j.apenergy.2023.121768 (2023).

48. Sheng, W. et al. Short-term load forecasting algorithm based on LST-TCN in power distribution network. *Energies* **15**, 5584. https://doi.org/10.3390/en15155584 (2022).
49. Das, K., Kumar, R. & Krishna, A. Analyzing electric vehicle battery health performance using supervised machine learning. *Renew. Sustain. Energy Rev.* **189**, 113967. https://doi.org/10.1016/j.rser.2023.113967 (2024).
50. Liu, K. et al. Remaining useful life prediction for lithium-ion batteries based on sliding window technique and Box-Cox transformation. *J. Energy Storage* **74**, 109352. https://doi.org/10.1016/j.est.2023.109352 (2023).
51. Yin, W. et al. Study on orderly charging strategy of EV with load forecasting. *Energy* **278**, 127818. https://doi.org/10.1016/j.energy.2023.127818 (2023).
52. Liu, X. Bi-level planning method of urban electric vehicle charging station considering multiple demand scenarios and multi-type charging piles. *J. Energy Storage* **48**, 104012. https://doi.org/10.1016/j.est.2022.104012 (2022).

Author contributions
All authors contributed to the study conception and design. Conceptualization, Methodology, Dexin Gao and Yuanming Cheng; Writing–Original Draft, Yuanming Cheng; Software, Investigation, Validation, Yuanming Cheng and Fengming Zhao; Resources, Supervision, Dexin Gao and Qing Yang; Writing–Review and Editing, Dexin Gao and Yuanming Cheng; Funding Acquisition, Dexin Gao.

Funding
This research was funded by the Key Research and Development Program of Shandong Province of China (Grant No. 2019GGX101012).

Declarations

Competing interests
The authors have no competing interests to declare that are relevant to the content of this article.

Ethical approval
The data used in this study was exclusively generated by the authors. No third parties were involved in the data generation. No research involving human participants or animals has been performed.

Additional information
Correspondence and requests for materials should be addressed to D.-X.G.

Reprints and permissions information is available at www.nature.com/reprints.

Publisher's note Springer Nature remains neutral with regard to jurisdictional claims in published maps and institutional affiliations.

Open Access This article is licensed under a Creative Commons Attribution-NonCommercial-NoDerivatives 4.0 International License, which permits any non-commercial use, sharing, distribution and reproduction in any medium or format, as long as you give appropriate credit to the original author(s) and the source, provide a link to the Creative Commons licence, and indicate if you modified the licensed material. You do not have permission under this licence to share adapted material derived from this article or parts of it. The images or other third party material in this article are included in the article's Creative Commons licence, unless indicated otherwise in a credit line to the material. If material is not included in the article's Creative Commons licence and your intended use is not permitted by statutory regulation or exceeds the permitted use, you will need to obtain permission directly from the copyright holder. To view a copy of this licence, visit http://creativecommons.org/licenses/by-nc-nd/4.0/.

© The Author(s) 2025